Supplementary Information for Imaging physics-driven artificial intelligence makes ground-based telescope resolve deep field universe

Yan Lu[1,2], Hao Du[1], Jiaze Li[1,3], Kuo-Cheng Wu[1], Zhen Wan[5], Guohang Zhuang[1,6], Yating Liu[1,4], Shixiang Tang[1,2], Lei Bai[1], Bin Liu[3], Zhijian Luo[7], Zhu Chen[7], Shiyin Shen[8], Renhao Ye[8], Wanli Ouyang[1,2,9]

[1]*Center of AI for Science, Shanghai Artificial Intelligence Laboratory, Shanghai 200233, China*

[2]*Department of Information Engineering, the Chinese University of Hong Kong, Hong Kong, China*

[3]*School of Information Science and Technology, University of Science and Technology of China, Hefei, Anhui 230026, China*

[4]*School of Artificial Intelligence and Data Science, University of Science and Technology of China, Hefei, Anhui 230026, China*

[5]*School of Astronomy and Space Science, University of Science and Technology of China, Hefei 230026, China*

[6]*School of Computer Science and Information Engineering, Hefei University of Technology, Anhui 230009, China*

[7]*Shanghai Key Lab for Astrophysics, Shanghai Normal University, Shanghai 200234, China*

[8]*Shanghai Astronomical Observatory, Chinese Academy of Sciences, Shanghai 200030, China*

[9]*Shenzhen Loop Area Institute, Shenzhen 015000, China*

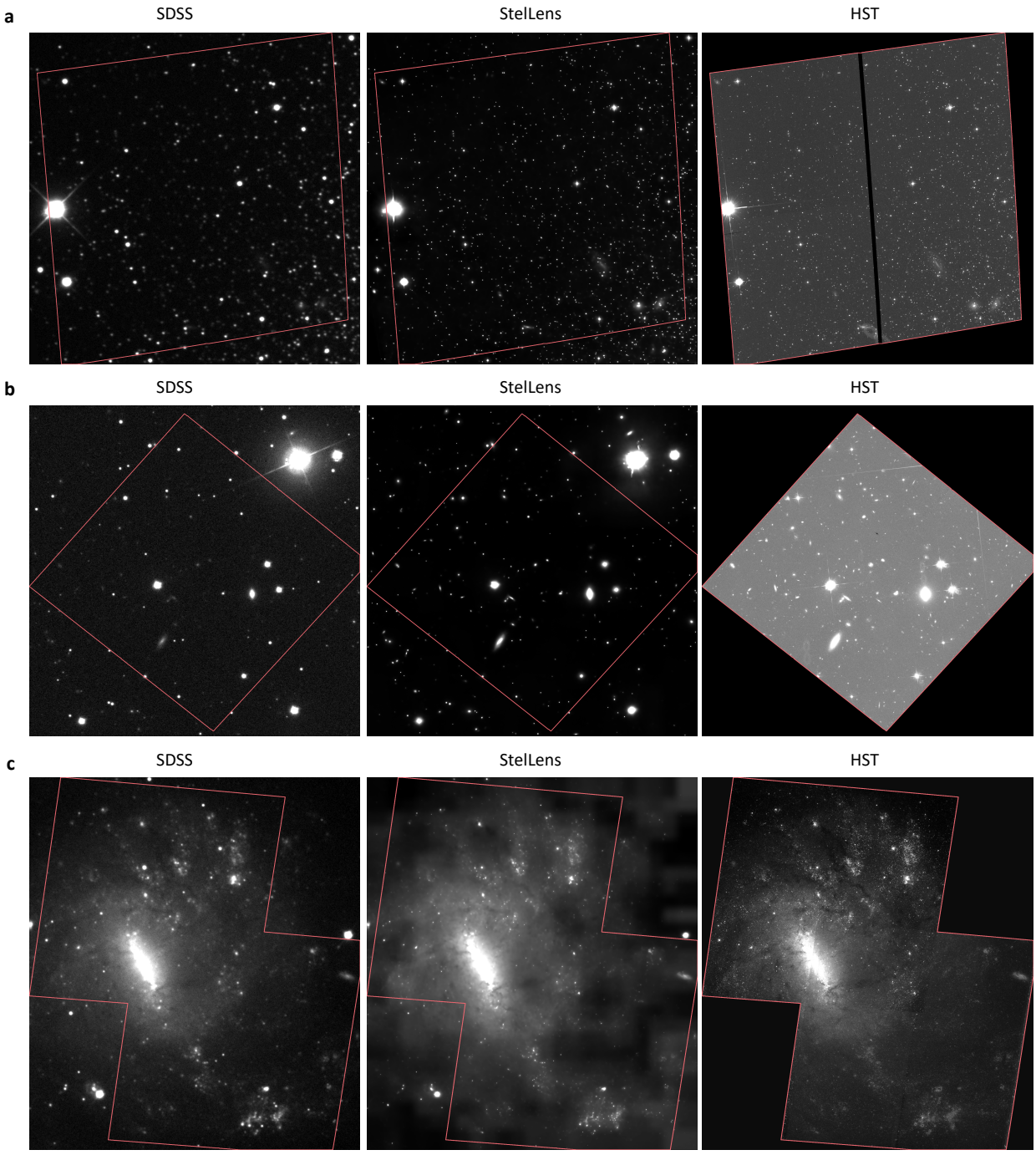

Extended Data Fig. 1: **More visualizations between SDSS, StelLens, and HST.** Note that SDSS and StelLens images are geometrically aligned with HST for comparison. The red line indicates the image range captured by HST. The RA and DEC of the three cases are: **a**, $\mathrm{RA} = 322.581249°,\ \mathrm{DEC} = 12.103835°$; **b**, $\mathrm{RA} = 319.604877°,\ \mathrm{DEC} = 0.287639°$; **c**, $\mathrm{RA} = 199.716185°,\ \mathrm{DEC} = -21.038105°$. These cases demonstrate that StelLens effectively narrows the resolution gap between ground-based and space-based images and reveals faint structures with greater clarity.

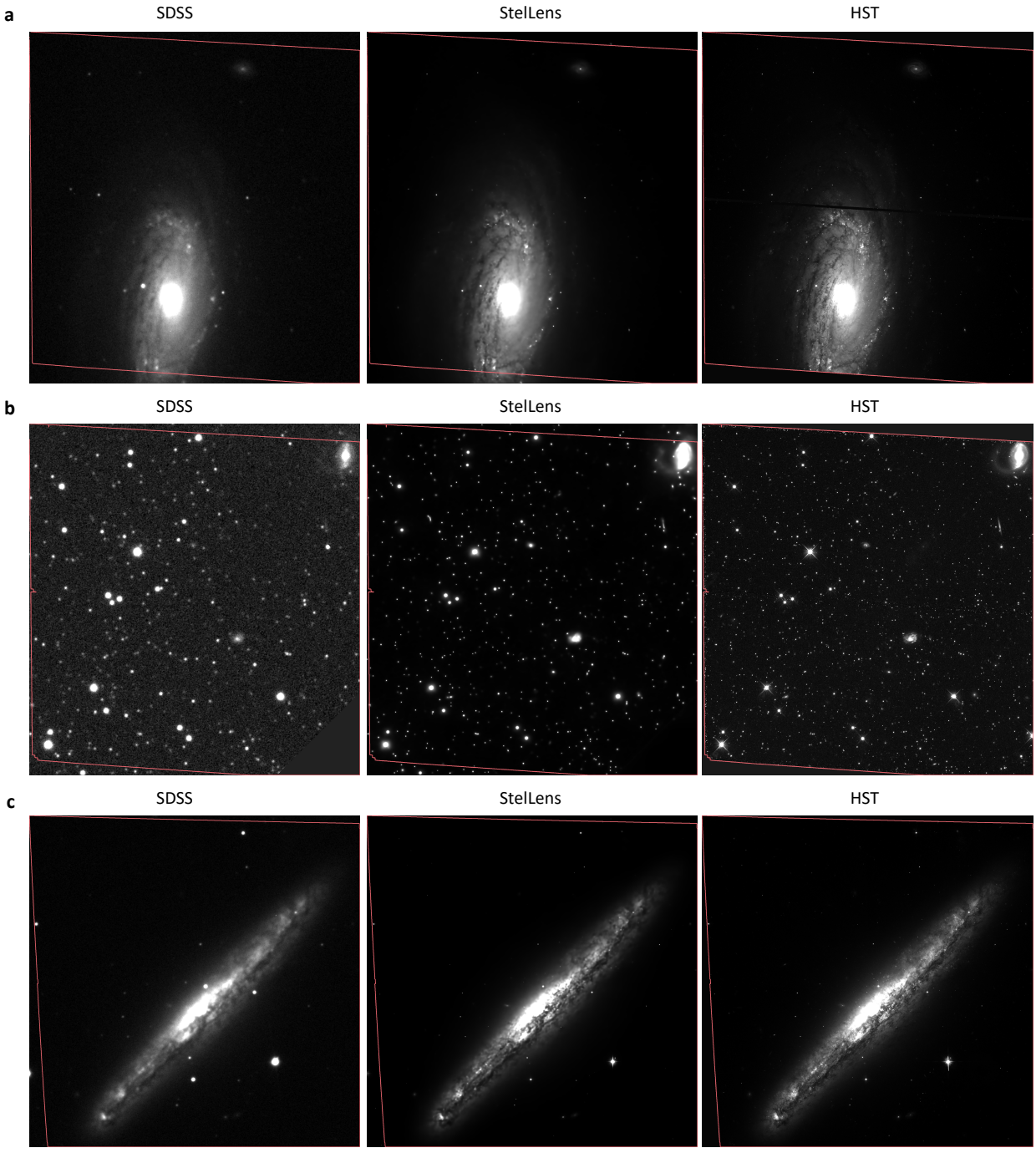

Extended Data Fig. 2: **More visualizations between SDSS, StelLens, and HST.** Note that SDSS and StelLens images are geometrically aligned with HST for comparison. The red line indicates the image range captured by HST. The RA and DEC of the three cases are: **a**, RA $= 225.004103°$, DEC $= 1.867464°$; **b**, RA $= 229.032929°$, DEC $= -0.143275°$; **c**, RA $= 223.472788°$, DEC $= 3.546616°$. These cases demonstrate that StelLens effectively narrows the resolution gap between ground-based and space-based images and reveals faint structures with greater clarity.

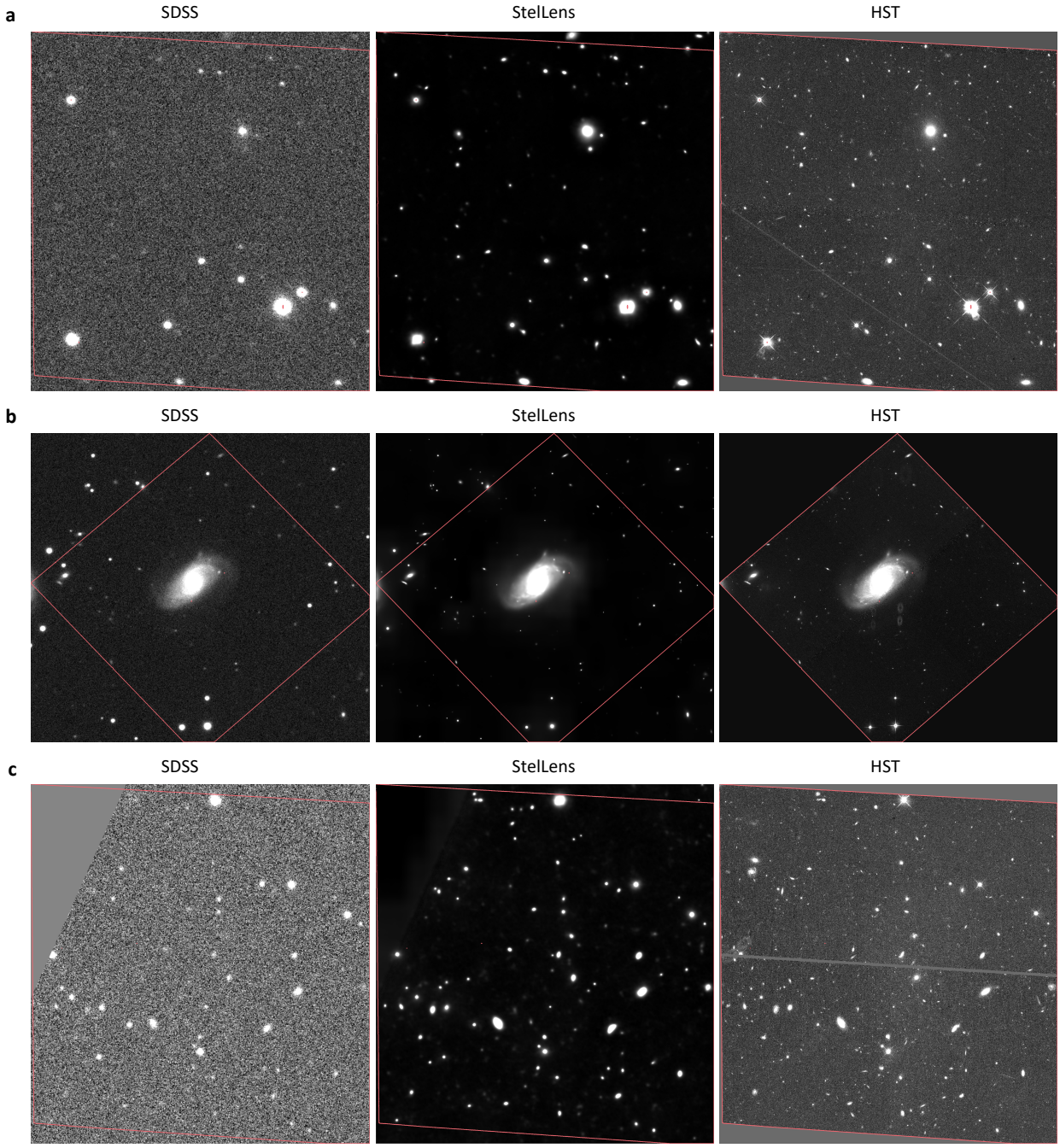

Extended Data Fig. 3: **More visualizations between SDSS, StelLens, and HST.** Note that SDSS and StelLens images are geometrically aligned with HST for comparison. The red line indicates the image range captured by HST. The RA and DEC of the three cases are: **a**, $\mathrm{RA} = 205.408715°$, $\mathrm{DEC} = -3.373336°$; **b**, $\mathrm{RA} = 226.483612°$, $\mathrm{DEC} = 3.709689°$; **c**, $\mathrm{RA} = 205.702024°$, $\mathrm{DEC} = -0.616524°$. These cases demonstrate that StelLens effectively narrows the resolution gap between ground-based and space-based images and reveals faint structures with greater clarity.

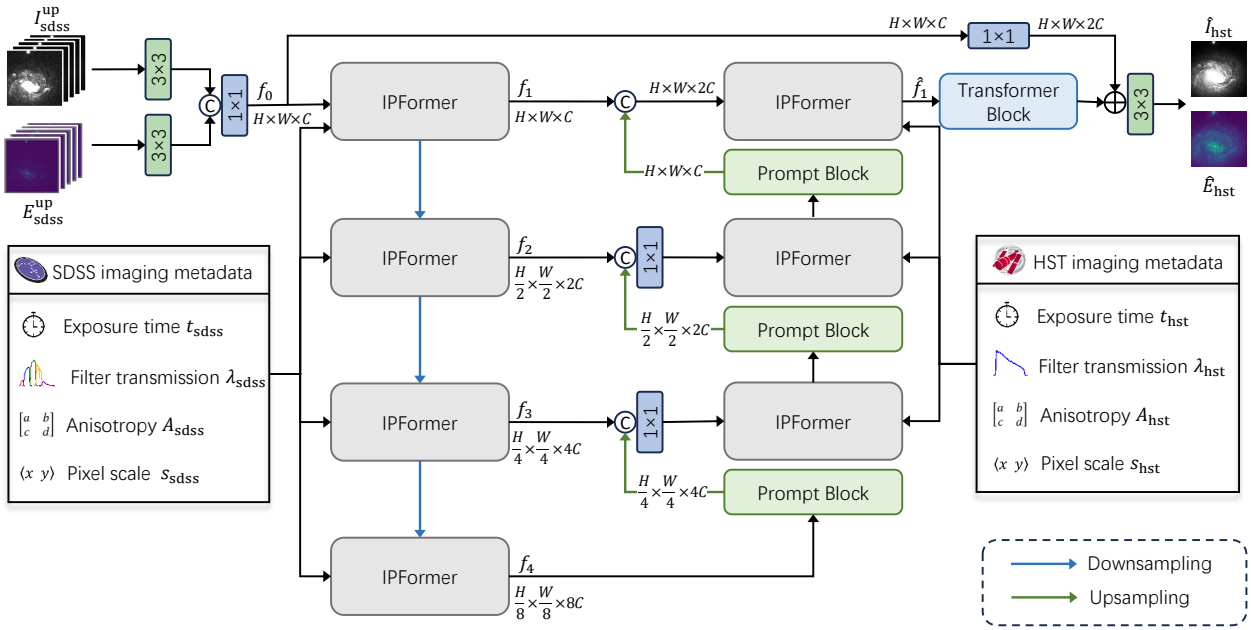

Extended Data Fig. 4: **StelLens model details.** The arrows indicate the flow of information among the different components described in the Restoration Model Structure.

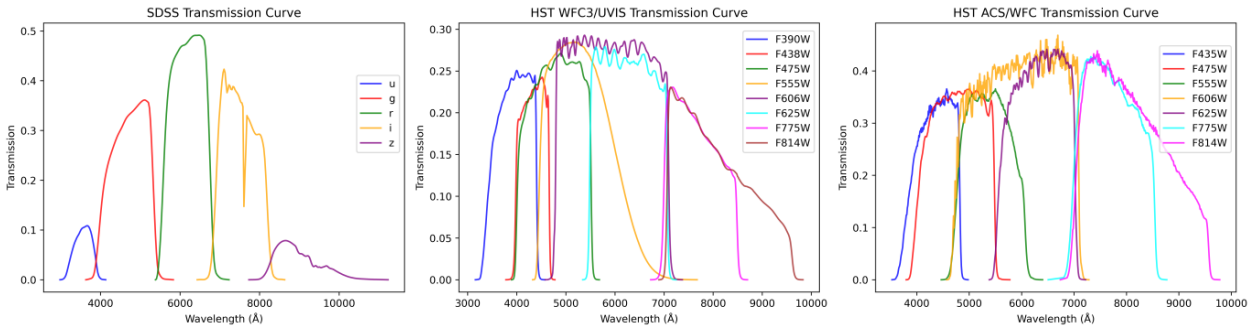

Extended Data Fig. 5: **Filter visualizations.** The left panel displays the transmission curve of the five bands in SDSS, while the middle and right panels show the transmission curves of different filters for the HST instruments WFC3/UVIS and ACS/WFC, respectively. This demonstrates that the HST filters we selected overlap with the SDSS $ugriz$ bands, eliminating the ill-posed property.

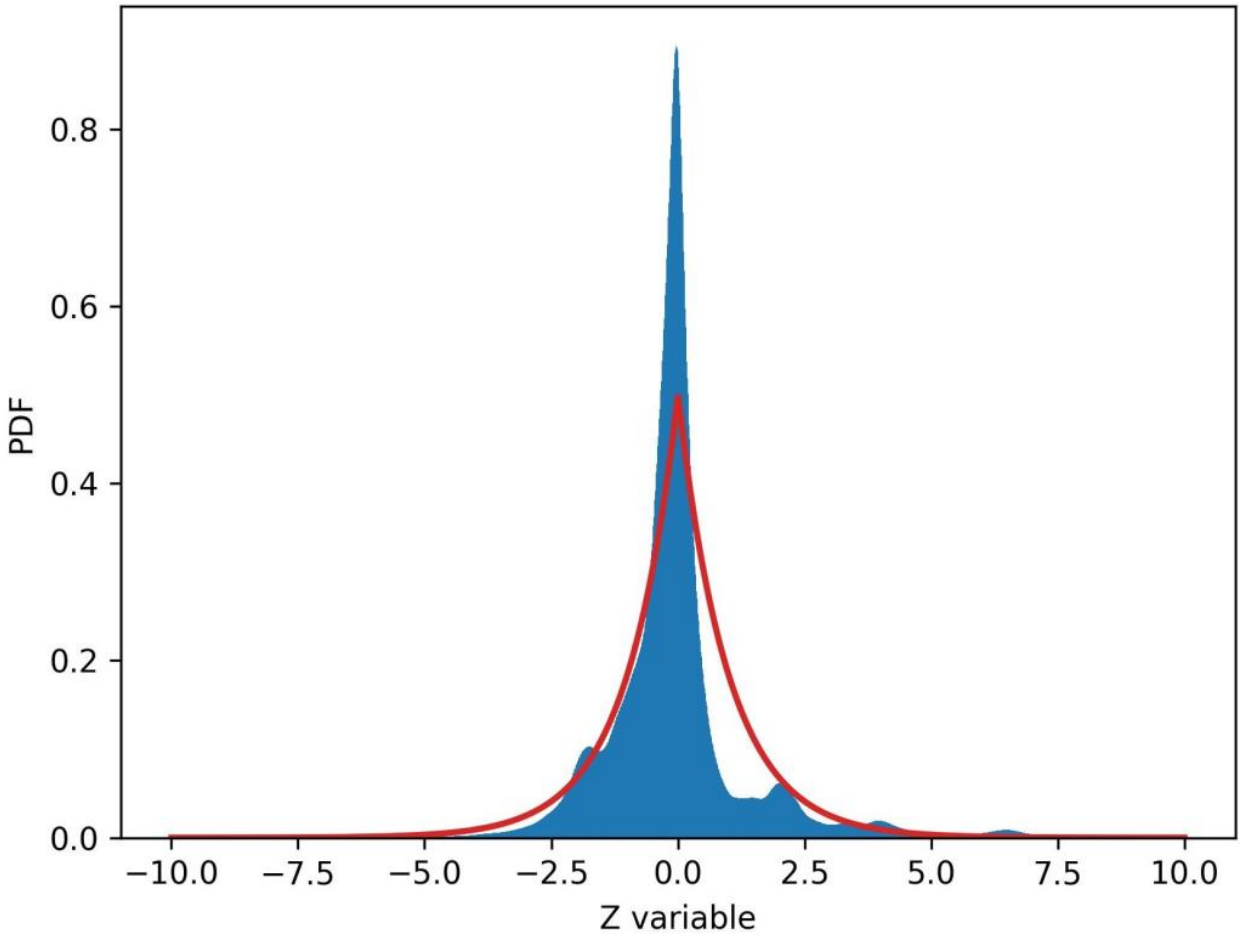

Extended Data Fig. 6: **Uncertainty estimation.** The blue bins show the histogram of the normalized z variables, while the red curve denotes the probability density function (PDF) of the standard Laplacian distribution, corresponding to the base assumption of EC-NLL (see Methods for details). The close agreement between the histogram and the reference curve indicates that the predicted uncertainties are well calibrated.

Extended Data Table 1: **Ablation Studies.**

	NLL	EC-NLL	Transformer Encoder	Transformer Decoder	IPFormer Encoder	IPFormer Decoder	MSSIM ↑	$\widetilde{\chi}^2$ ↓
(a)	✓	–	✓	✓	–	–	0.646	60.09
(b)	–	✓	✓	✓	–	–	0.642	57.19
(c)	–	✓	–	✓	✓	–	0.741	56.04
(d)	–	✓	✓	–	–	✓	0.828	53.40
(e)	–	✓	–	–	✓	✓	**0.832**	**52.44**

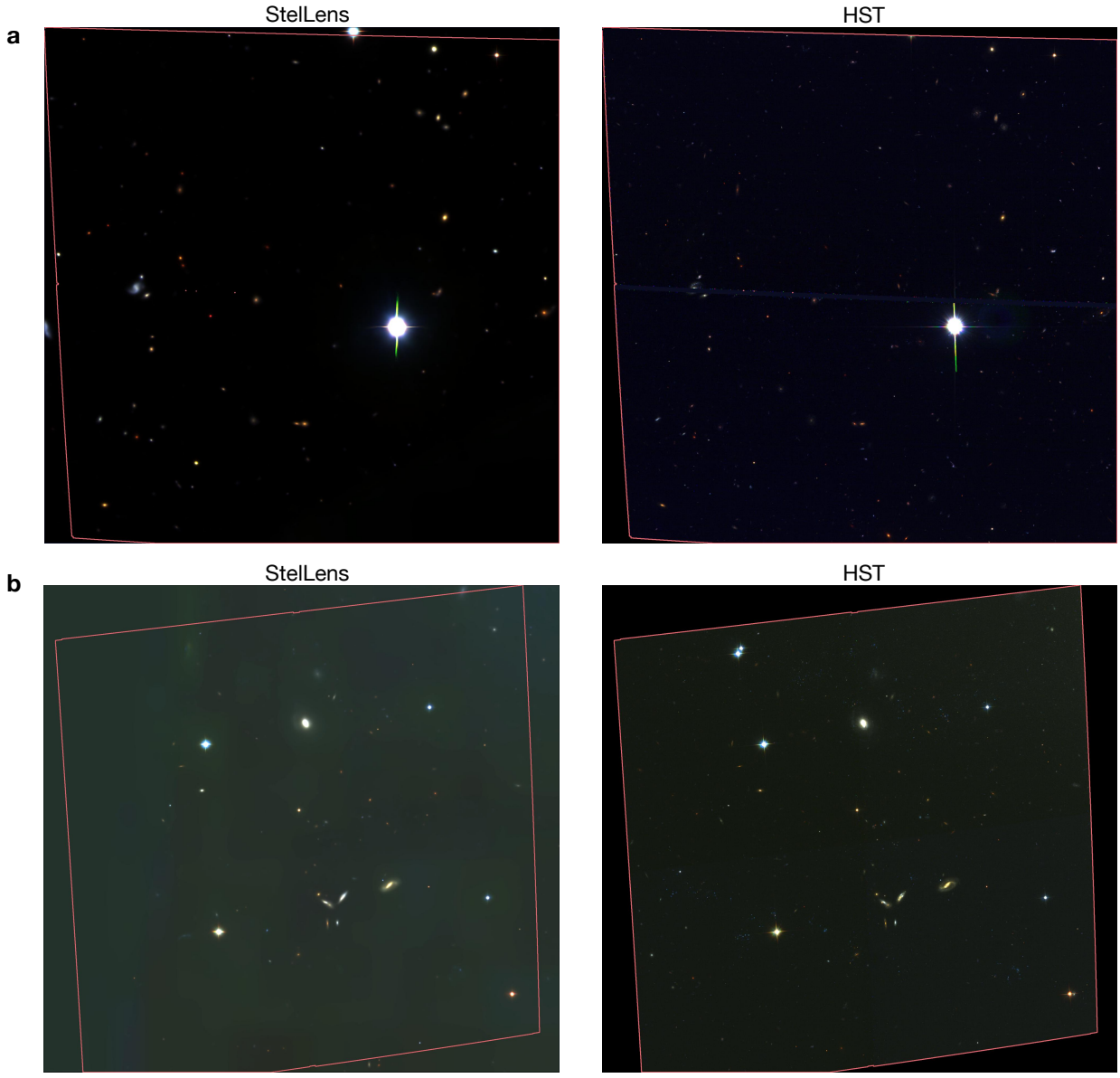

Extended Data Fig. 7: **More multi-band visualizations.** Two more galaxy field RGB synthetic image examples of StelLens and HST. The red rectangle outlines the HST coverage within the SDSS field. The RA and DEC of the two examples are: **a**, RA $= 189.094688°$, DEC $= 62.400346°$; **b**, RA $= 199.078461°$, DEC $= 42.099574°$.